

Photophysiological acclimation of *Phaeocystis antarctica* Karsten under light limitation

Tiffany A. Moisan and B. Greg Mitchell

Marine Research Division, Scripps Institution of Oceanography, University of California, La Jolla, California 92093-0218

Abstract

Primary production models and pigment algorithms for remote optical systems including satellites, moorings, or drifters depend on an improved understanding of the relationship between spectral light absorption, pigments, and photosynthesis for species of phytoplankton that are widespread and numerically abundant. Cultures of colonial *Phaeocystis antarctica*, a prymnesiophyte that can dominate the phytoplankton community in the Southern Ocean, were grown under blue light at seven different levels ranging from 14 to 542 $\mu\text{mol quanta m}^{-2} \text{s}^{-1}$ at 4°C under nutrient-replete conditions. Chlorophyll-specific absorption (a_{ph}^*) at 436 nm increased linearly from 0.03 to 0.11 $\text{m}^2 \text{mg chlorophyll } a^{-1}$ with increasing light intensities. This variability is attributed to pigment packaging effects and pigmentation. The 2.5-fold range in the values of a_{ph}^* (676 nm) demonstrates significant pigment packaging effects due to the intracellular pigment content, single cell diameter within the colony, and thylakoid stacking. Quantum yield for growth (ϕ_{μ}) varied 30-fold, ranging from 0.003 to 0.09 mol carbon fixed (mol quanta absorbed) $^{-1}$. Under low light conditions, the relatively high ϕ_{μ} and high $a_{\text{ph}}^*(\lambda)$ may enable *Phaeocystis* to accumulate a seed population to initiate blooms at the beginning of spring when light levels are low, mixed layers are deep, and sea ice is still significant. These aspects of its photophysiology may contribute to the ecological success of *Phaeocystis* in polar regions.

The genus *Phaeocystis* is a numerically and functionally important component in polar biogeochemical cycles. Mesoscale blooms of *Phaeocystis* appear to be frequent and widespread in polar and subpolar seas (Weisse et al. 1994; Stoecker et al. 1996), and single cells can be numerically important during austral winter (Moisan unpubl. data). *Phaeocystis* blooms in coastal and ice edge regions are at times substantial enough to deplete macronutrients in surface waters (Smith et al. 1991; van Boeckel et al. 1992). In addition to its ecological importance, dimethylsulfide production by *Phaeocystis* may be a significant contributor to the sulfur cycle (Liss et al. 1994). Dimethylsulfide can be rapidly oxidized to sulfate aerosols in the atmosphere, which can serve as cloud condensation nuclei that may change cloud albedo (Charlson et al. 1987).

Phaeocystis exhibits a heteromorphic life history, which alternates between free-living flagellated zoospores and a gelatinous aggregation of nonmotile palmelloid cells arranged in a spherical colony (Rousseau et al. 1994). Alternating life cycle phases between 3- μm single cells and millimeter-size colonies allow *Phaeocystis* to serve as a food source to a wide size range of predators (Rousseau et al. 1994; Weisse et al. 1994). A significant portion of the primary production may be directed toward bacteria at the end of a bloom by release of dissolved organic carbon through excretion and

cell lysis, which may be more important than particulate carbon transfer through predation (van Boeckel et al. 1992). Alternatively, *Phaeocystis* blooms can sink to the ocean's interior or sediments at the termination of the bloom (Wassman et al. 1990). Thus *Phaeocystis*, when abundant, may affect carbon transfer in the polar food web and biogeochemical cycle.

Oceanographers have approached the goal of estimating primary production through remote sensing by the use of semianalytical and simple regression models that compare phytoplankton pigments with primary production (Balch et al. 1989; Behrenfeld and Falkowski 1997). Many contemporary models (Kiefer and Mitchell 1983; Sakshaug et al. 1989; Cullen 1990) utilize the chlorophyll-specific absorption coefficient $a_{\text{ph}}^*(\lambda)$ and quantum yield for growth ϕ_{μ} as photophysiological parameters in models of net primary production,

$$P_{\text{net}} = \text{Chla} \int_{350\text{nm}}^{700\text{nm}} \phi_{\mu} a_{\text{ph}}^*(\lambda) E_o(\lambda) d\lambda. \quad (1)$$

Symbols are defined in Table 1.

To better parameterize a model for primary production in polar regions and understand the underlying physiological mechanisms that control the variables within the models, the absorption characteristics and photophysiology must be estimated for species that are widespread and capable of dominating blooms. The key photophysiological parameters in primary production models, $a_{\text{ph}}^*(\lambda)$ and $\phi(\lambda)$, have been characterized in the laboratory for relatively few and mostly temperate phytoplankton species. Previous studies have shown that cell size, thylakoid stacking, quantity, and type of pigment per cell vary with growth conditions, including temperature, light, and nutrients (Cleveland and Perry 1987; Nelson and Prézélin 1990; Sosik and Mitchell 1991, 1995). Results of these studies demonstrate that variations in cellular properties and acclimation of the photosynthetic apparatus lead to variability in $a_{\text{ph}}^*(\lambda)$ and $\phi_{\mu}(\lambda)$.

Acknowledgments

We thank Scott Cheng for his excellent technical assistance, Robert A. Anderson for providing the culture, Steve Barlow for unending patience with TEM preparations, and Miguel Olaiola and Ralf Goericke for assistance with HPLC analysis and thoughtful discussions regarding pigment data. We thank Geir Johnsen for the discussions on a_{cm} . Comments by Maria Vernet, Heidi Sosik, Paul G. Falkowski, and an anonymous reviewer greatly improved the manuscript. We thank J. L. Swan for formatting assistance. Support for this work was provided by ONR grant N00014-91-J-1186 to B.G.M. and a NASA Earth System Science Fellowship NGT 5-30036 to T.A.M.

Table 1. Symbols used throughout the text.

PSI	Photosystem I
PSII	Photosystem II
P_{net}	Net primary production
λ	Wavelength (nm)
Chl	Chlorophyll
F_{DCMU}	In vivo DCMU-enhanced fluorescence (relative units)
μ	Specific growth rate (d^{-1})
C	Particulate carbon ($\mu\text{g l}^{-1}$)
N	Particulate nitrogen ($\mu\text{g l}^{-1}$)
$E_o(\lambda)$	Spectral quantum scalar irradiance ($\mu\text{mol quanta m}^{-2} \text{s}^{-1}$)
$E'(\lambda)$	Relative spectral quantum irradiance
PAR	Photosynthetically available radiation defined as $\int_{350\text{nm}}^{700\text{nm}} E_o(\lambda) d\lambda$ ($\mu\text{mol quanta m}^{-2} \text{s}^{-1}$)
C_i	Concentration of pigment i (mg m^{-3})
$a_i(\lambda)$	Weight-specific absorption spectrum of pigment i ($\text{m}^2 \text{mg}^{-1}$)
$a_{\text{ph}}(\lambda)$	Absorption by phytoplankton (m^{-1})
$a_{\text{cm}}(\lambda)$	Absorption by cellular material (m^{-1})
$a_{\text{ph}}^*(\lambda)$	Chlorophyll-specific absorption of phytoplankton ($\text{m}^2 \text{mg Chl } a^{-1}$)
$a_{\text{ps}}^*(\lambda)$	Chlorophyll-specific absorption due to photosynthetic pigments ($\text{m}^2 \text{mg Chl } a^{-1}$)
$a_{\text{pp}}^*(\lambda)$	Chlorophyll-specific absorption due to photoprotective pigments ($\text{m}^2 \text{mg Chl } a^{-1}$)
$a_{\text{cm}}^*(\lambda)$	Chlorophyll-specific absorption of cellular material ($\text{m}^2 \text{mg Chl } a^{-1}$)
ϕ_{μ}	Quantum yield for growth ($\text{mol C fixed} [\text{mol quanta absorbed}]^{-1}$)
ϕ_{m}	Maximal quantum yield ($\text{mol C fixed} [\text{mol quanta absorbed}]^{-1}$)
$\phi_{\text{m}E_o}$	Maximal quantum yield at a steady state irradiance ($\text{mol C fixed} [\text{mole quanta absorbed}]^{-1}$)
σ	Absorption cross section of PSII ($\text{m}^2 [\text{mol photosynthetic unit}]^{-1}$)
τ	Turnover time of the photosynthetic electron transport system (h)
α	Photosynthetic efficiency ($\text{mg C} [\text{mg Chl } a]^{-1} \text{h}^{-1} [\mu\text{mol quanta m}^{-2} \text{s}^{-1}]^{-1}$)
$E_{k\mu}$	Saturation irradiance for growth ($\mu\text{mol quanta m}^{-2} \text{s}^{-1}$)
Q_a	Absorption efficiency, dimensionless
Q_a^*	Pigment packaging parameter, dimensionless
ρ'	Optical thickness along the particle diameter, dimensionless
d	Diameter of single cell within colony (m)

Because light is one of the main factors limiting phytoplankton growth and the onset of blooms in polar regions, cultures of colonial *Phaeocystis antarctica* Karsten were grown under nutrient-replete conditions at irradiances ranging from limiting to photoinhibiting for photosynthesis. We present here photophysiological characteristics that may contribute to the ecological success of *Phaeocystis* during spring blooms in polar waters and model parameterizations to predict $a_{\text{ph}}^*(\lambda)$ and ϕ_{μ} based on irradiance.

Materials and methods

Cultures of *Phaeocystis antarctica* (CCMP 1374) were grown semicontinuously for five to eight generations in *f/2*

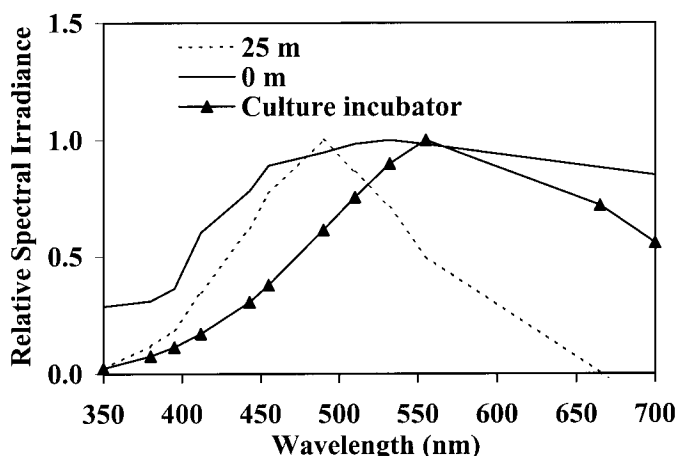


Fig. 1. Comparison between the relative spectral quantum irradiance used in the culture incubator and California coastal waters at 0 and 25 m. Spectra are normalized to 1.0 at their respective peaks. Symbols represent discrete points where irradiance was estimated.

medium (Guillard and Ryther 1962) at 4°C. Bubbled cultures were diluted with medium to ensure they were nutrient replete and “optically thin.” Cultures were grown under continuous blue light ranging from 14 to 542 $\mu\text{mol quanta m}^{-2} \text{s}^{-1}$. Four 500-W tungsten halogen lamps were transmitted through a blue theatre gel (Roscolux 720), spectrally neutral perforated nickel screens (Stork Veco), a water-filled aquarium, and a 1:1 glycol:water temperature-controlled mixture. The spectrum attained with this system was similar to that of ocean surface waters (Fig. 1). The oceanic spectral irradiance is dependent on depth, particles, colored dissolved organic matter, and sea ice cover.

Irradiance was determined with a PAR scalar irradiance meter (Biospherical Instruments QSL-100) inside culture vessels filled with distilled water. The relative spectral irradiance was measured with a MER2040 (Biospherical Instruments) at 13 discrete wavelengths. These spectral data were transformed from relative energy to relative quantum flux, linearly interpolated at 1-nm intervals, and used to spectrally scale PAR, allowing an estimate of scalar spectral quantum irradiance,

$$E_o(\lambda) = \frac{\text{PAR} \cdot E'(\lambda)}{\int_{350\text{nm}}^{700\text{nm}} E'(\lambda) d\lambda}. \quad (2)$$

Chlorophyll-specific absorption coefficient—In vivo whole cell absorption spectra ($n = 4$) were determined at 1-nm intervals with an integrating sphere accessory in a dual beam spectrophotometer (Perkin Elmer Lambda 6 UV/Vis). Fresh *f/2* medium was used as a reference and as a blank. The chlorophyll-specific absorption coefficient was estimated by dividing \log_e absorption, $a_{\text{ph}}(\lambda)$, by the corresponding fluorometric chlorophyll *a* (Chl *a*) value:

$$a_{\text{ph}}^*(\lambda) = a_{\text{ph}}(\lambda) [\text{Chl } a]^{-1}. \quad (3)$$

Sample preparation of a_{cm} —Cells were unpackaged by a modification of the technique developed by Johnsen et al. (1994). Cells were disrupted three times with a French press at 1.37×10^8 Pa, and the slurry was centrifuged at $10,000 \times g$. Absorption spectra of the supernatant ($n = 2$) were measured in an integrating sphere (Perkin Elmer Lambda 6) and processed as described above for $a_{ph}^*(\lambda)$. A volume of $100 \mu\text{l}$ was added to 90% acetone, and Chl *a* was estimated fluorometrically. Chlorophyllase activity was assumed to be minimal, as has been documented for *Phaeocystis* (Jeffrey and Hallegraeff 1987).

Fluorescence excitation spectra—Spectra ($n = 3$) were obtained at ambient growth temperatures with a spectrofluorometer (Spex Fluoromax) at 1-nm resolution with the emission monochromator set at 730 nm (Neori et al. 1988) with a 20-nm emission band width. The chemical, 3-(3,4-dichlorophenyl)-1,1 dimethyl urea (DCMU) was added to cultures to remove photochemical quenching of variable fluorescence; therefore, we refer to this variable as $F_{DCMU}(\lambda)$. Spectra were run in sample-to-reference mode and corrected for the excitation quantum flux using 2,7-bis-(diethylamino) phenazonium perchlorate (Kopf and Heinz 1984). To estimate the chlorophyll-specific absorption by photosynthetically active pigments (a_{ps}^* , Sosik and Mitchell 1995), $F_{DCMU}(\lambda)$ was scaled to $a_{ph}^*(676 \text{ nm})$ at the red peak:

$$a_{ps}^*(\lambda) = \frac{F_{DCMU}(\lambda)a_{ph}^*(676 \text{ nm})}{F_{DCMU}(676 \text{ nm})}. \quad (4)$$

Specific growth rate, cell size, and cell concentrations—Specific growth rate (μ) was estimated by a linear regression of \log_e -transformed daily determinations of in vivo fluorescence intensity ($n = 2$) measured with a fluorometer (Turner Model 10). Individual cell size ($n = 25$) was determined at a magnification of $1,000\times$ on samples preserved with a final concentration of 2% glutaraldehyde (Fryxell and Kendrick 1983), which dissolved the colonial matrix of *Phaeocystis*. Cell concentrations were estimated in Palmer Maloney chambers at a magnification of $400\times$.

Particulate carbon and nitrogen content—Samples ($n = 3$) were filtered onto precombusted filters, stored at -20°C , and run on a carbon analyzer (Perkin Elmer). Acetanilide was used as an external standard.

High-performance liquid chromatography and spectral reconstruction of $a_{ph}(\lambda)$ —Samples ($n = 2$) were concentrated onto Whatman GF/F filters and extracted in cold 100% acetone by grinding with a teflon-tip grinding rod. Cleared samples were combined with 20% (v/v) high-performance liquid chromatography (HPLC)-grade water and analyzed on an HPLC system (Shimadzu LC10-AD) (Wright et al. 1991). Pigment concentrations were based on absorption at 440 nm (Dynamax Model UV-1). Integrated HPLC peak area was quantified with external standards. Canthaxanthin was used as an internal standard.

Reconstructed values of $a_{ph}(\lambda)$ were estimated as the product of the corrected in vivo weight-specific absorption co-

efficient of the major pigments, $a_i^*(\lambda)$, given by Bidigare et al. (1990) and their volume-based HPLC concentrations (C_i):

$$a_{ph}^*(\lambda) = \sum a_i(\lambda) * C_i. \quad (5)$$

*Fluorometric estimates of Chl *a**—Chl *a* concentrations ($n = 3$) were estimated fluorometrically (Yentsch and Menzel 1963). We normalized a_{ph} to fluorometric Chl *a* estimates because of the limited culture volumes. To be consistent, fluorometric Chl *a* estimates were used for all other normalizations relating to cellular characteristics. HPLC and fluorometric values for Chl *a* differed from 5% to 20% of each other.

Transmission electron microscopy—Cells were fixed on ice with a 2% glutaraldehyde and 1.3% osmium tetroxide solution for 30 min and rinsed in distilled water. Cells were dehydrated through a series of ethanol:water washes (25:75, 50:50, 75:25, 95:5), three washes of 100% ethanol, and three washes of 100% acetone. Cells were stained with uranyl acetate and lead citrate. Chloroplasts ($n = 30$) were examined with a Philips 410 transmission electron microscope at $14,500\times$ or $17,000\times$ magnification. Thylakoid stacks were quantified on negatives by counting them along a transect normal to thylakoids in the middle of the chloroplast (Berner et al. 1989). This technique assumes a symmetry in the distribution of the thylakoids across and within the plastid.

Quantum yield for growth—Quantum yield for growth was based on the carbon-specific growth rate, the whole cell in vivo spectral absorption, and the spectral irradiance in each treatment (Sosik and Mitchell 1991, 1995).

Results and discussion

Variability in $a_{ph}^(\lambda)$ due to light limitation*—The in vivo whole cell absorption properties of *Phaeocystis* varied in response to the growth irradiance. Chlorophyll-specific absorption, $a_{ph}^*(\lambda)$, increased with light intensity (Fig. 2A). Chlorophyll-specific absorption at the blue peak, $a_{ph}^*(436 \text{ nm})$, increased linearly with light intensity from 0.031 to $0.107 \text{ m}^2 \text{ mg Chl } a^{-1}$ (Table 2, Fig. 2B). At the red peak, $a_{ph}^*(676 \text{ nm})$ varied from 0.012 to $0.030 \text{ m}^2 \text{ mg Chl } a^{-1}$. Values of $a_{ph}^*(490 \text{ nm})$ ranged from 0.020 to $0.068 \text{ m}^2 \text{ mg Chl } a^{-1}$. An ultraviolet-B peak due to mycosporine-like amino acids was also observed for each treatment, with higher values at high light (data not shown). The ratio of $a_{ph}^*(436 \text{ nm})$ to $a_{ph}^*(676 \text{ nm})$ varied from 1.8 to 3.7 but did not show a consistent trend with light (Table 2). Our values of $a_{ph}^*(676 \text{ nm})$ agree well with other reports for Chl *a-c*-containing eukaryotic phytoplankton (Nelson and Prézelin 1990; Sakshaug et al. 1991; Johnsen et al. 1994). Our observations are within the range of absorption observed during a *Phaeocystis* bloom; Cota et al. (1994) found that a_{ph}^* averaged $0.056 \pm 0.07 \text{ m}^2 \text{ mg Chl } a^{-1}$ and $0.023 \pm 0.011 \text{ m}^2 \text{ mg Chl } a^{-1}$ in the blue and red peaks, respectively.

Pigment package effects in Phaeocystis—Because changes in $a_{ph}^*(\lambda)$ at the red peak are minimally dependent on changes

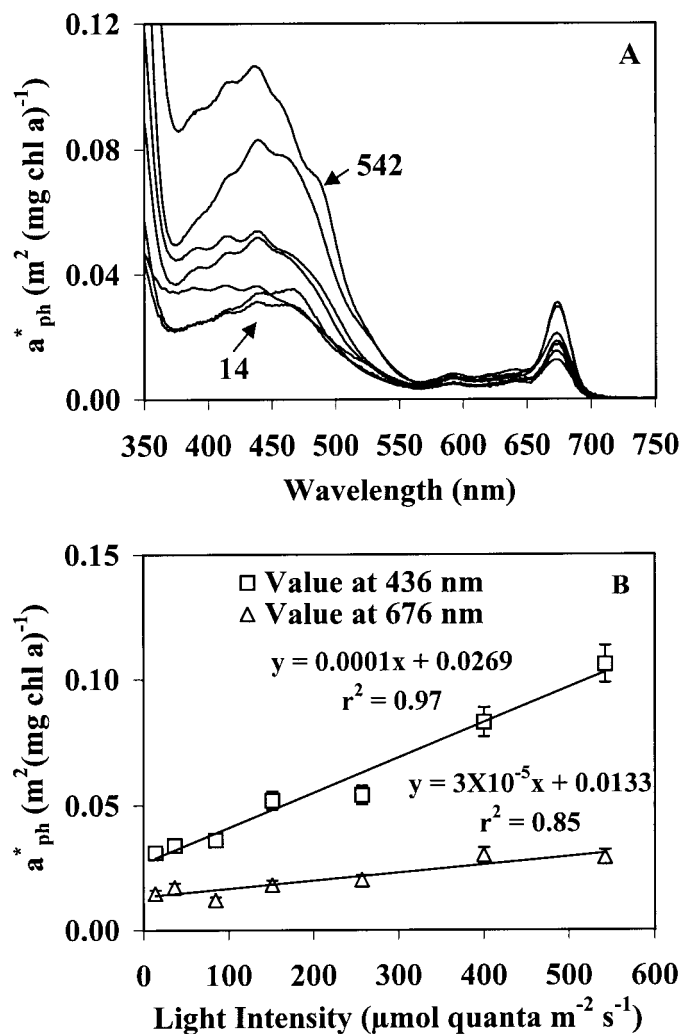


Fig. 2. (A) In vivo chlorophyll-specific absorption for *Phaeocystis* grown between 14 and 542 $\mu\text{mol quanta m}^{-2} \text{s}^{-1}$ at 4°C under nutrient-replete conditions. (B) Linear relationship of a_{ph}^* (436 and 676 nm) to light intensity. $n = 4 \pm \text{SE}$.

in accessory pigments, the approximate 2.5-fold change in a_{ph}^* (676 nm) is attributed to pigment package effects. The effects of pigment packaging were assessed by comparing a_{ph}^* (676 nm) to an unpackaged suspension, a_{cm}^* (676 nm), prepared with a French press, which mechanically disrupts cells without decoupling pigment-protein complexes (Johnsen et al. 1994). Under low light (14 $\mu\text{mol quanta m}^{-2} \text{s}^{-1}$), *Phaeocystis* demonstrated a significant pigment packaging effect; values of a_{cm}^* (676 nm) were $0.023 \pm 0.0009 \text{ m}^2 \text{ mg Chl } a^{-1}$, and a_{ph}^* (676 nm) values were reduced by about half, $0.01 \pm 0.001 \text{ m}^2 \text{ mg Chl } a^{-1}$ (Fig. 3A). In contrast, *Phaeocystis* cells demonstrated less of a pigment packaging effect at the higher light intensities (259 $\mu\text{mol quanta m}^{-2} \text{s}^{-1}$); values of a_{cm}^* (676 nm) were $0.029 \pm 0.003 \text{ m}^2 \text{ mg Chl } a^{-1}$, and values of a_{ph}^* (676 nm) were $0.020 \pm 0.0005 \text{ m}^2 \text{ mg Chl } a^{-1}$ (Fig. 3B).

At both irradiances, a_{cm}^* was greater than a_{ph}^* in the region between 550 and 650 nm, where pigment packaging effects are expected to be minimal because of weak absorption (Kirk 1994). This finding may be a residual artifact due to incomplete removal of small ($<0.1 \mu\text{m}$) French-press micelles. Scattering errors in absorption will be minimal at the red peak where pigment packaging effects were assessed because small particles scatter inefficiently at the longer wavelengths.

To assess the cellular characteristics responsible for pigment packaging effects, cellular properties such as Chl *a* per volume, cell size, and thylakoid stacking were examined. Specific growth rates ranged from 0.04 to 0.34 d^{-1} (Table 2). The C:N ratios showed no trend with light intensity; they were similar to those found by Cota et al. (1994) during a nutrient-replete oceanic bloom and were lower than those found by Wassman et al. (1990) during a nutrient-limited bloom. Chl *a* per cell was low at the higher light intensities and increased as *Phaeocystis* acclimated to lower light (Table 2, Fig. 4A). Cellular Chl *a* values in this study are in the range reported for *Phaeocystis* by Baumann et al. (1994, 0.10–1.68 pg Chl *a* per cell). The diameter of individual *Phaeocystis* cells ranged from $3.4 \pm 0.67 \mu\text{m}$ to 5.1 ± 0.95

Table 2. Growth, cell, and photosynthetic characteristics of *Phaeocystis* grown under seven irradiances at 4°C under nutrient-replete conditions. Average coefficient of variation is given for estimates.

	Irradiance ($\mu\text{mol quanta m}^{-2} \text{s}^{-1}$)						
	14	37	84	151	259	400	542
μ (d^{-1})*	0.04	0.12	0.19	0.24	0.25	0.34	0.29
C:N ratio (w:w)†	NA‡	5.94	6.28	6.12	6.22	5.66	6.13
pg Chl <i>a</i> cell ⁻¹ †	0.39	0.45	0.41	0.36	0.36	0.27	0.19
Diameter (μm)*	3.7	3.5	3.4	3.6	3.8	4.2	5.1
a_{ph}^* (436 nm)§	0.031	0.033	0.036	0.051	0.054	0.082	0.107
a_{ph}^* (676 nm)	0.014	0.017	0.012	0.018	0.020	0.030	0.029
a_{ph}^* (490 nm)	0.020	0.022	0.021	0.031	0.035	0.053	0.068
a_{ph}^* (436:676 nm)	2.1	1.8	3.3	2.5	2.5	2.8	3.7
a_{ph}^* (436 nm)§	NA	NA	0.03	0.04	0.04	0.06	0.05
ϕ_{μ}	NA	0.09	0.09	0.03	0.007	0.006	0.002
ϕ_{mEo}	NA	0.109	0.127	0.050	0.018	0.021	0.012

* Coefficient of variation (CV) = 7%.

† CV = 10%.

‡ NA = est. not available.

§ CV = 5%.

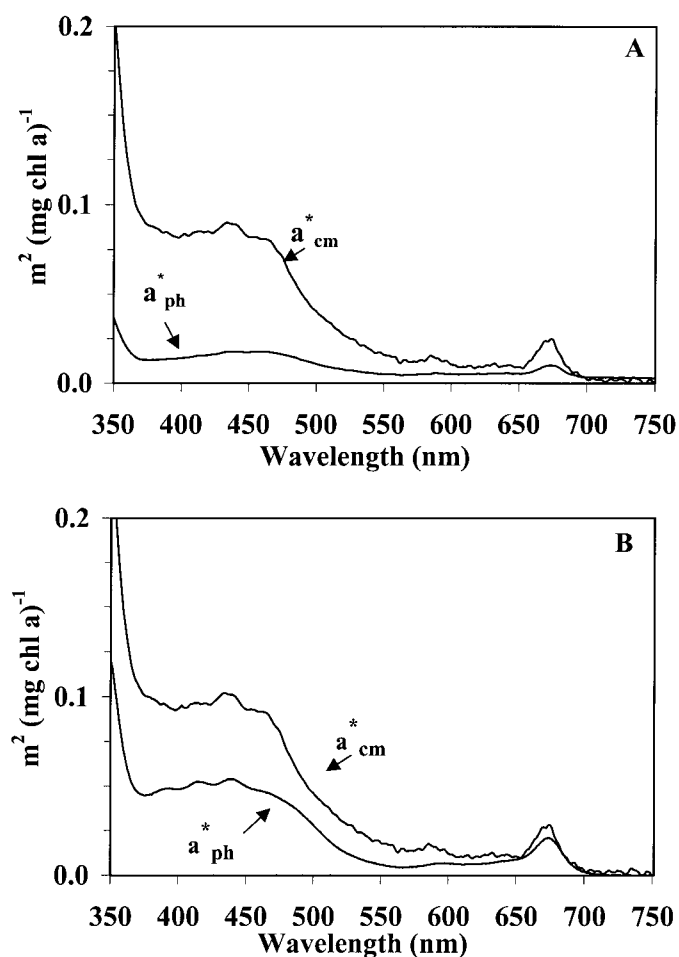


Fig. 3. Comparison between unpackaged chlorophyll-specific absorption, $a_{cm}^*(\lambda)$, and whole cell chlorophyll-specific absorption, $a_{ph}^*(\lambda)$, for *Phaeocystis* grown at 14 (A) and 259 (B) $\mu\text{mol quanta m}^{-2} \text{s}^{-1}$.

m (Table 2, Fig. 4B). Both the decrease in cell size and the increase in Chl *a* per cell at lower light contributed to a stronger increase in Chl *a* per cellular volume (Fig. 4A,B).

Under low-light acclimation, the increased pigment per cell increases the cellular absorption cross-section, which leads to pigment packaging and results in less efficient absorption per mass of pigment. By reducing cell diameter at low light in response to increased cellular pigment, *Phaeocystis* minimizes pigment packaging effects. These results can be interpreted on the basis of Mie theory as applied to phytoplankton (Morel and Bricaud 1986), which assumes that the cells are spherical and pigments are homogeneously distributed. There are deviations from Mie theory in non-spherical cells (Kirk 1976). The Morel and Bricaud (1986) theory predicts the absorption efficiency (Q_a) and the pigment packaging parameter (Q_a^*) as a function of the dimensionless parameter (ρ'):

$$\rho' = a_{cm}d, \quad (6)$$

where d is the diameter of a single cell (m) and a_{cm} is the unpackaged absorption coefficient of the cellular material (m^{-1}) as estimated from a French press preparation (Johnsen

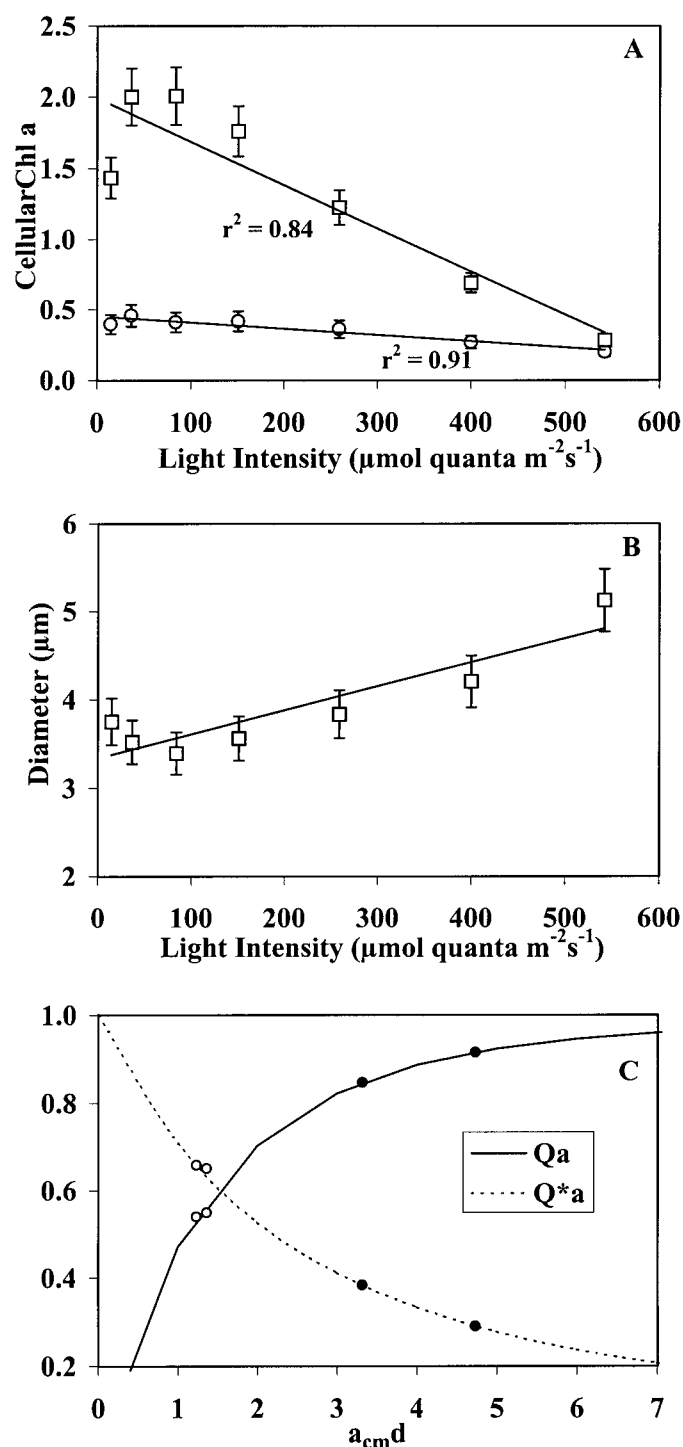


Fig. 4. Cell characteristics. (A) Mean \pm SE pg Chl *a* cell $^{-1}$ (circles) and pg Chl *a* (μm^3) $^{-1} \times 10$ (squares). (B) Mean \pm SE single cell diameter. (C) In vivo absorption efficiency (Q_a) and the theoretical packaging parameter (Q_a^*) at the red (open) and blue (solid) absorption peaks as a function of ρ' for *Phaeocystis* grown at 14 and 259 $\mu\text{mol quanta m}^{-2} \text{s}^{-1}$. Solid and dashed lines are the theoretical functions and were calculated with Eqs. 7 and 8. The value of a_{cm} was determined by the method of Johnsen et al. (1994). Cell diameter was determined by microscopy.

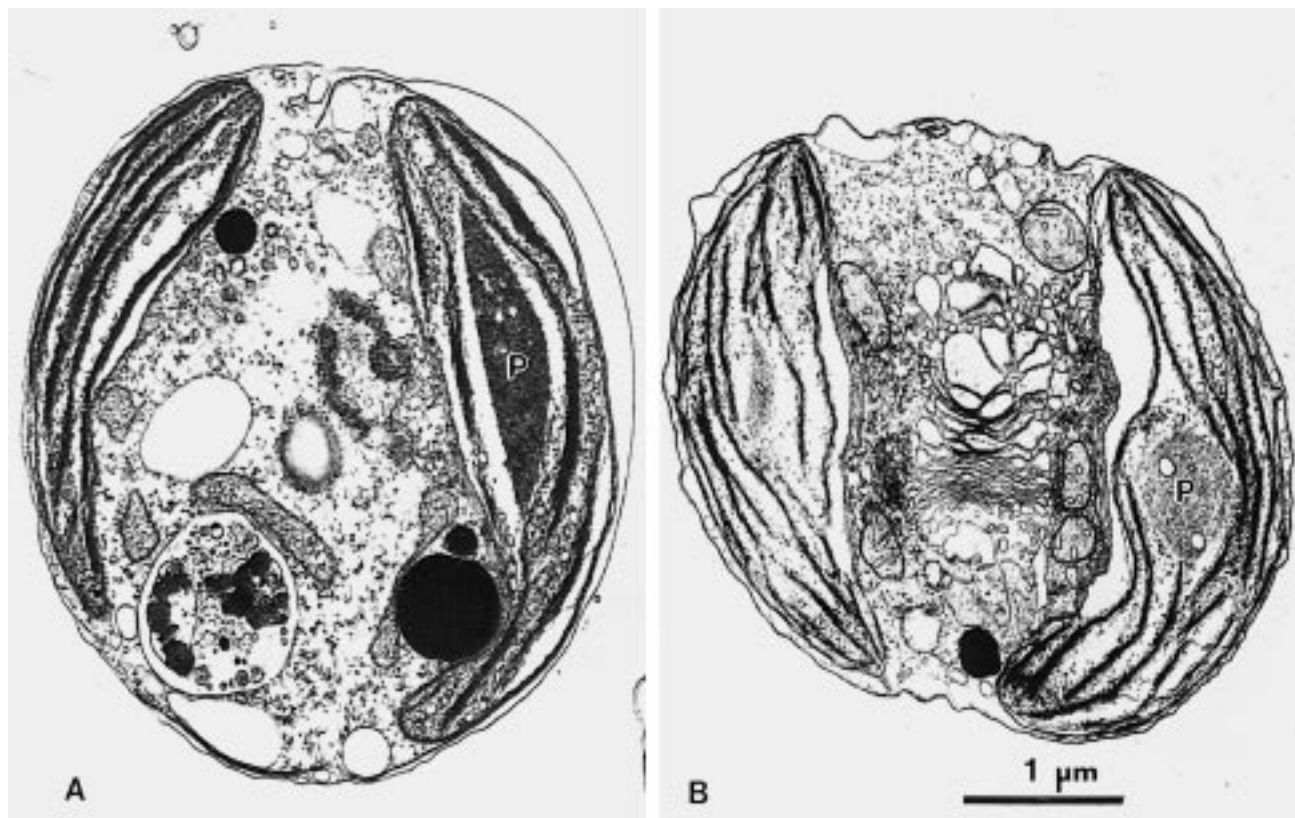


Fig. 5. Transmission electron micrographs of *Phaeocystis* single cells grown under 259 (A) and 14 (B) $\mu\text{mol quanta m}^{-2} \text{s}^{-1}$. P = pyrenoids.

et al. 1994). The theory predicts that Q_a increases nonlinearly as ρ' increases and approaches an asymptote as ρ' increases, as given by the following equation:

$$Q_a(\lambda) = 1 + \frac{2 \exp - \rho'(\lambda)}{\rho'(\lambda)} + 2 \frac{[\exp - \rho'(\lambda) - 1]}{\rho'(\lambda)^2}. \quad (7)$$

The pigment packaging parameter, Q_a^* is related to Q_a as given by the following equation,

$$Q_a^*(\lambda) = \frac{3 Q_a(\rho')}{2 \rho'}. \quad (8)$$

Figure 4C shows the results of this study and the theoretical curves of Q_a and Q_a^* . By decreasing its diameter while pigment per volume increases at low light (Fig. 4A,B), *Phaeocystis* minimizes the pigment packaging effects ordinarily associated with low-light acclimation (Mitchell and Kiefer 1988). The energetic investment of having greater cellular pigment per cell in order to increase absorption at low light is made more efficient because of the decreased cell size, which minimizes the package effect (Morel and Bricaud 1986). Still, at the lowest light intensities, a_{ph}^* at 676 nm was 2.5 times lower than it was at high light, which indicates strong pigment package effects. Even stronger package effects occur in the vicinity of the blue peak, which has more absorption than the red peak.

Although Mie theory provides a useful framework for understanding cellular optical properties, real cells do not conform to the Mie assumption of internally homogenous

spheres. Actual subcellular absorption is accomplished in the chloroplast. Therefore, the variability of thylakoid stacking within the two parietal chloroplasts of *Phaeocystis* was examined. Berner et al. (1989) estimated that thylakoid stacking can contribute to about 40% of the change in the pigment packaging effect and to 20% of the overall change in $a_{\text{ph}}^*(\lambda)$. To evaluate the effects of light intensity on thylakoid stacking, cultures were grown at a limiting (14 $\mu\text{mol quanta m}^{-2} \text{s}^{-1}$) and a saturating irradiance (259 $\mu\text{mol quanta m}^{-2} \text{s}^{-1}$). At high light, 3.6 ± 1.0 thylakoid stacks per chloroplast were observed, and the pyrenoid was a significant portion of the chloroplast volume (Fig. 5A). In contrast, *Phaeocystis* grown under low light conditions had an average of 6.5 ± 1.6 thylakoid stacks per chloroplast, and the pyrenoid did not take up a significant portion of the chloroplast volume (Fig. 5B). We did not resolve the number of thylakoids per stack, but ultrastructural studies of prymnesiophytes have demonstrated that there are three thylakoids per stack (Gibbs 1970). Although the pyrenoid has low absorption in the visible portion of the spectrum, it may contribute to some scattering effects within the chloroplast that could enhance absorption by pigment-protein complexes through path length amplification, which could in theory account for part of the increase in $a_{\text{ph}}^*(\lambda)$ at high light.

Pigmentation in *Phaeocystis*—In addition to assessing the contribution of pigment packaging effects to the variability in $a_{\text{ph}}^*(\lambda)$, we also examined cellular pigmentation, which ul-

Table 3. Pigmentation (pg cell⁻¹) of *Phaeocystis* grown at 4°C under nutrient-replete conditions. Photosynthetic pigments (PS) include chlorophyll (Chl), 19'-hexanoyloxyfucoxanthin (19'-hex), and fucoxanthin (Fuco). Photo-protective pigments (PP) include diadinoxanthin (DD), β -carotene, and diatoxanthin (DT). HPLC and fluorometric (fluor) Chl *a* values are compared.

Light intensity μmol quanta $\text{m}^{-2} \text{s}^{-1}$	Chl <i>a</i>		Chl ($c_1 + c_2$)	Chl c_3	19'-hex	Fuco	β -carotene	DD + DT	Total pigment per cell	Fraction of total pigment (w : w)	
	Fluor	HPLC								PS	PP
14	0.39	0.37	0.12	0.031	0.23	0.0028	0.0012	0.006	0.76	0.99	0.01
37	0.46	0.44	0.14	0.036	0.28	0.0138	0.0011	0.007	0.92	0.99	0.01
84	0.41	0.49	0.12	0.032	0.13	0.0050	0.0049	0.035	0.82	0.95	0.05
151	0.36	0.33	0.09	0.022	0.12	0.0039	0.0038	0.033	0.61	0.94	0.06
259	0.36	0.37	0.11	0.027	0.14	0.0034	0.0041	0.029	0.69	0.95	0.05
400	0.27	0.29	0.06	0.019	0.09	0.0120	0.0046	0.035	0.50	0.92	0.08
542	0.19	0.15	0.02	0.007	0.04	0.0023	0.0043	0.057	0.28	0.78	0.22

timately affects the magnitude and spectral shape of $a_{\text{ph}}^*(\lambda)$. The predominant pigments found in this study are in agreement with previous findings for Chl c_3 prymnesiophytes with the exception that 19'-butanoyloxyfucoxanthin was not observed. Our cellular pigment values were slightly lower than those found by Vaulot et al. (1994) but are within the range found by Buma et al. (1991) for a variety of *Phaeocystis* culture strains.

Total pigment per cell was inversely related to light intensity and ranged from 0.28 to 0.92 pg cell⁻¹ (Table 3). Chl *a* was the dominant light-harvesting pigment followed by 19'-hexanoyloxyfucoxanthin, Chl ($c_1 + c_2 + c_3$), and fucoxanthin; these pigments together comprised 99% of the total weight of cellular pigment at low light and accounted for approximately 78% at the higher light intensity (w : w; Table 3, Fig. 6A). At the higher light intensities, the amount of diadinoxanthin and photoprotective pigments, such as β -carotene and diatoxanthin, per cell increased in relative importance, ranging from 1% to 22% of the total pigment weight (Table 3, Fig. 6A), with higher values at high light.

Contribution of pigmentation to $a_{\text{ph}}^(\lambda)$* —The contribution of each pigment to the magnitude of $a_{\text{ph}}^*(\lambda)$ is equal to the product of the volume-based HPLC concentration and the in vivo pigment-specific absorption coefficient. In vivo absorption coefficients of unpackaged individual pigments are not well characterized for microalgae and higher plants. Instead, we used in vitro absorption coefficients (Bidigare et al. 1990) to reconstruct $a_{\text{ph}}(\lambda)$. This technique does not take into account pigment packaging effects and has unresolved issues regarding spectral shape and molar in vivo absorption coefficients. Despite these problems, the method allowed us to assess the relative importance of pigmentation to $a_{\text{ph}}(\lambda)$ and $a_{\text{ph}}^*(\lambda)$ at low light (Fig. 6B) and high light (Fig. 6C).

At the red peak, Chl *a* is the only pigment that contributes significantly to a_{ph}^* (676 nm). Between 400 nm and 500 nm, different pigments dominate at different wavelengths. Cellular Chl *a* contributed most to the variability of a_{ph} (436 nm) at all of the light intensities, mainly because of its high cellular concentration even though it has a relatively low weight-specific absorption coefficient at 436 nm (Bidigare et al. 1990). The relative importance of pigments to a_{ph} (436

nm) was followed by Chl ($c_1 + c_2 + c_3$) and 19'-hexanoyloxyfucoxanthin. Fucoxanthin contributed very little to the magnitude of a_{ph} (436 nm). At a_{ph}^* (490 nm), 19'-hexanoyloxyfucoxanthin made up the largest fraction (w : w) of pigments that absorb at this wavelength and contributed to the variability in $a_{\text{ph}}(\lambda)$ at 14 and 37 μmol quanta $\text{m}^{-2} \text{s}^{-1}$. The increased concentration of 19'-hexanoyloxyfucoxanthin is most notable in the increase in the ratio of a_{ph} (490 nm) to a_{ph} (436 nm) at the low light intensities (Fig. 2A). At light intensities above 37 μmol quanta $\text{m}^{-2} \text{s}^{-1}$, the pool of diadinoxanthin and diatoxanthin contributed more to the variability, and the contribution of 19'-hexanoyloxyfucoxanthin to a_{ph} (490 nm) was less significant as compared with the lower light treatment. The pigment reconstruction methodology suggests that the relative contribution of pigments in *Phaeocystis* varies with irradiance and affects the overall shape of $a_{\text{ph}}^*(\lambda)$. However, the pigment reconstruction method does not provide a satisfactory quantitative estimate of true in vivo absorption (Sosik and Mitchell 1991; Fig. 6B,C).

Estimation of photosynthetically active absorption—Haxo and Blinks (1950) originally normalized the photosynthetic action spectrum to an absorption spectrum to assess relative activity of pigments. Relative excitation spectra with emission monitored in the near infrared (730 nm) have been shown to exhibit spectral features similar to oxygen evolution action spectra (Neori et al. 1988). These observations have served as the basis for normalizing a fluorescence excitation spectrum to an absorption spectrum at the red peak as a proxy for photosynthetically active absorption, symbolized here as a_{ps}^* following Sosik and Mitchell (1995). The basis for this proxy resides in the ability of photosynthetic pigments to donate excitation energy to Chl *a*, which fluoresces at physiological temperatures, whereas photoprotective carotenoids either do not donate the absorbed energy or actually remove excitation energy from the pigment bed via thermal dissipation mechanisms (Owens 1991).

To estimate the amount of absorption that is photosynthetically active, a_{ps}^* is set to equal a_{ph}^* at the red peak because the action spectrum of Chl *a* fluorescence is assumed to be similar to the action spectrum for photosynthesis. We are not concerned with transfer efficiency to PSII but only whether

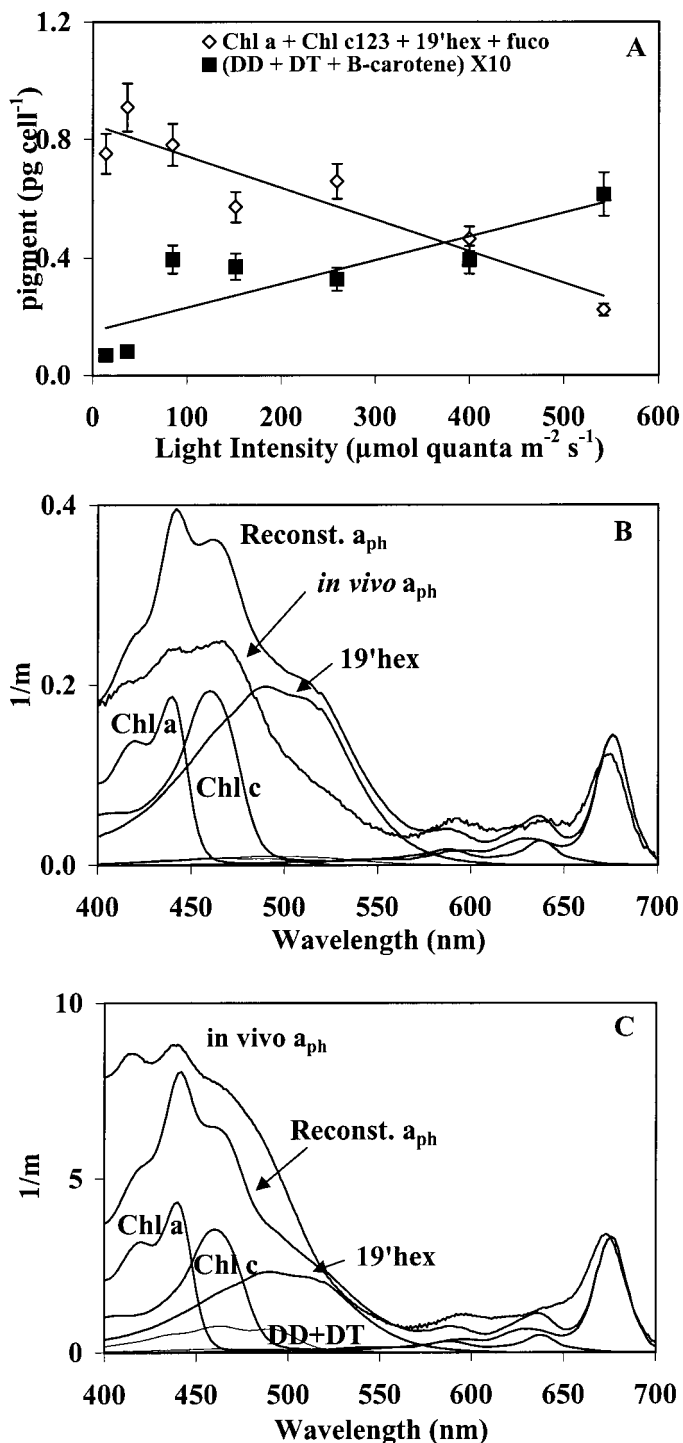


Fig. 6. (A) Amount of light-harvesting and photoprotective pigment per cell. Reconstructed $a_{ph}(\lambda)$ (Bidigare et al. 1990), *in vivo* $a_{ph}(\lambda)$, and contribution of major pigments (labeled) to the reconstructed $a_{ph}(\lambda)$ of cultures acclimated to 37 (B) and 259 (C) $\mu\text{mol quanta m}^{-2} \text{s}^{-1}$. β -Carotene and fucoxanthin are minor contributors to $a_{ph}(\lambda)$. Diadinoxanthin (DD) + diatoxanthin (DT) are major contributors to $a_{ph}(\lambda)$ only during conditions of high light. For (B) and (C), units are arbitrary.

the relative fluorescence spectrum has the same shape as the true a_{ps}^* . Because this study is based on cultures grown under constant environmental conditions, we assume that balanced growth exists because cultures were grown for a sufficient period to balance excitation energy. A variety of mechanisms to balance excitation energy have been described for algae (reviewed by Falkowski and Raven 1997).

Our estimate of photosynthetic absorption by *Phaeocystis* (Fig. 7A–E) generally meets the basic criterion that $a_{ps}^*(\lambda) \leq a_{ph}^*(\lambda)$. Values for a_{ps}^* (436 nm) ranged from 0.03 to 0.06 $\text{m}^2 \text{mg Chl } a^{-1}$ and showed less variability than $a_{ph}^*(\lambda)$ (Table 2, Fig. 7A–E). The equation,

$$\frac{a_{pp}(\lambda)}{a_{ph}(\lambda)} = \frac{\int_{350\text{nm}}^{700\text{nm}} a_{ph}(\lambda) d\lambda - \int_{350\text{nm}}^{700\text{nm}} a_{ps}(\lambda) d\lambda}{\int_{350\text{nm}}^{700\text{nm}} a_{ph}(\lambda) d\lambda} \quad (9)$$

represents the fraction of absorbed energy dissipated by photoprotective pigments relative to total light absorbed by the cells. Figure 7F shows that the fraction of absorption due to photoprotective pigments is correlated with the ratio of HPLC-determined photoprotective pigments to total pigments.

Quantum yield for growth—Quantum yield for growth, ϕ_{μ} , defined as the molar ratio of carbon fixed for growth to the quanta absorbed, is a fundamental biophysical variable and is a critical parameter in bio-optical models of net photosynthesis (Eq. 1; Sosik 1996). Model estimates of photosynthesis for natural phytoplankton populations are highly sensitive to variability in quantum yield (Sosik 1996). Using our complete data set, and rearranging Eq. 1, quantum yield for growth was estimated as,

$$\phi_{\mu} = \frac{\mu}{\text{Chl:C} \int_{350\text{nm}}^{700\text{nm}} a_{ph}^*(\lambda) E_o(\lambda) d\lambda} \quad (10)$$

For our study, ϕ_{μ} ranged from 0.003 to 0.09 mol C (mol quanta absorbed)⁻¹ with a nonlinear dependence on irradiance (Fig. 8A). These values are in the range previously reported for *Phaeocystis*-dominated blooms (SooHoo et al. 1987; Cota et al. 1994; Carder et al. 1995).

It is likely that our observations of decreased quantum yields at high irradiances were partly due to increases in photoprotective pigments that do not transfer energy to the photosynthetic reaction centers and therefore lower quantum yield. This concept is supported by the observation of increased concentrations of photoprotective pigments with increased irradiance (Table 3, Fig. 6A) and the dependence of $a_{pp}(\lambda)/a_{ph}(\lambda)$ on the photoprotective pigment concentrations (Fig. 7F). Also, nonphotochemical quenching may contribute to decreases in quantum yield in nature because *Phaeocystis* exhibits xanthophyll cycling between diadinoxanthin and diatoxanthin in response to abrupt irradiance changes (Moisan et al. 1998). It is also likely that the photoinhibiting light intensities led to an uncoupling of electron transport and carbon fixation (Bidigare et al. 1989).

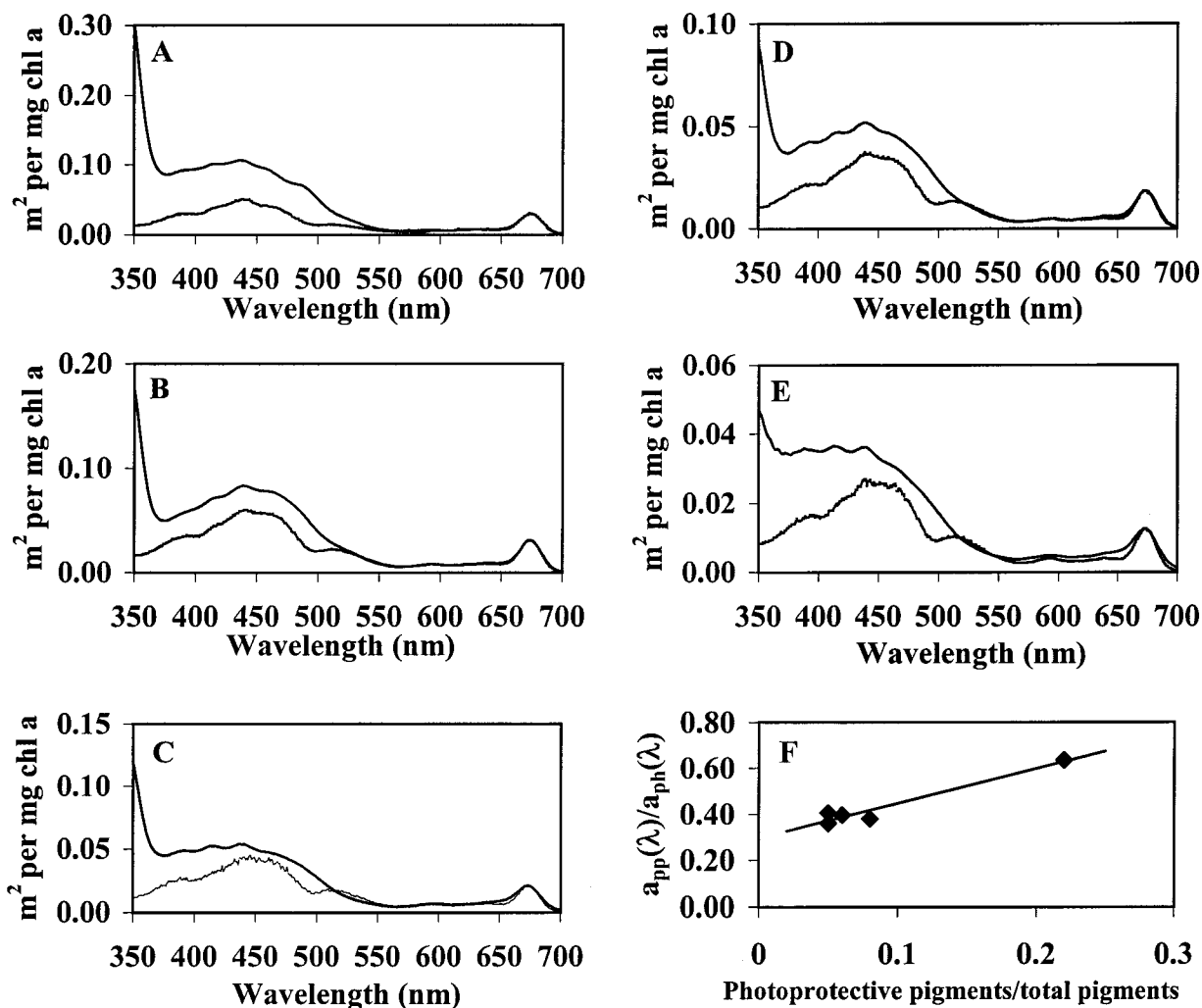


Fig. 7. Spectra of $a_{ps}^*(\lambda)$ (bottom curves) and $a_{ph}^*(\lambda)$ (top curves) at 542 (A), 400 (B), 259 (C), 151 (D), and 84 (E) $\mu\text{mol quanta m}^{-2} \text{s}^{-1}$. (F) $a_{app}(\lambda)/a_{ph}(\lambda)$ (Eq. 9) in relation to the fraction of photoprotective pigments of the total pigments.

Modeling quantum yield for growth—The quantum yield for photosynthesis has previously been modeled as a product of the maximal quantum yield for photosynthesis, ϕ_m , and a Poisson probability function that an open photosynthetic unit will be hit (Mauzerall 1978; Dubinsky et al. 1986). Sakshaug et al. (1989) adopted this concept to model the quantum yield for growth as

$$\phi_{\mu} = \phi_m \frac{1 - \exp^{-\sigma\tau E_o}}{\sigma\tau E_o}. \quad (11)$$

Sakshaug et al. (1989) used a constant ϕ_m and a constant, composite $\sigma\tau$ to represent the product of σ , the absorption cross section of PSII, and τ , the turnover time of the photosynthetic electron transport system. It has been shown on a mathematical basis that $\sigma\tau = E_k^{-1}$ (Cullen 1990; Falkowski and Raven 1997). We did not determine short-term P-E relationships, but our data do allow us to define the irradiance at which our *Phaeocystis* cultures are saturated for growth, which we refer to as $E_{k\mu}$. We normalized *Phaeocystis* growth rates from this study and from the literature to the maximum

rate observed in each study to remove nutrient and temperature effects. Relative growth rates (μ/μ_{max}) were plotted against irradiance to determine $E_{k\mu}$ (Fig. 8B). Using our study alone, the estimated $E_{k\mu}$ is 130 $\mu\text{mol quanta m}^{-2} \text{s}^{-1}$, and the overall composite of six separate studies provides a value of 110 $\mu\text{mol quanta m}^{-2} \text{s}^{-1}$. One might also expect that the $E_{k\mu}$ of *Phaeocystis* is temperature dependent, but this hypothesis needs further work.

We further propose that the ϕ_m used must be allowed to reflect realistic variability in the realized ϕ_m for a given set of environmental conditions. For example ϕ_m , which is determined from absorption and the initial slope of short-term P-E or flash yield experiments, has a different maximal quantum yield at a given light, nutrient, and temperature condition that is not necessarily the theoretical maximum of 0.125 mol C per mol quanta absorbed (Falkowski and Raven 1997). These ideal conditions are for achieving the maximal quantum yield, which is not necessarily (and generally is not) the ideal for maximal growth or maximal photosynthesis in a given environment. Thus, accurate modeling of quan-

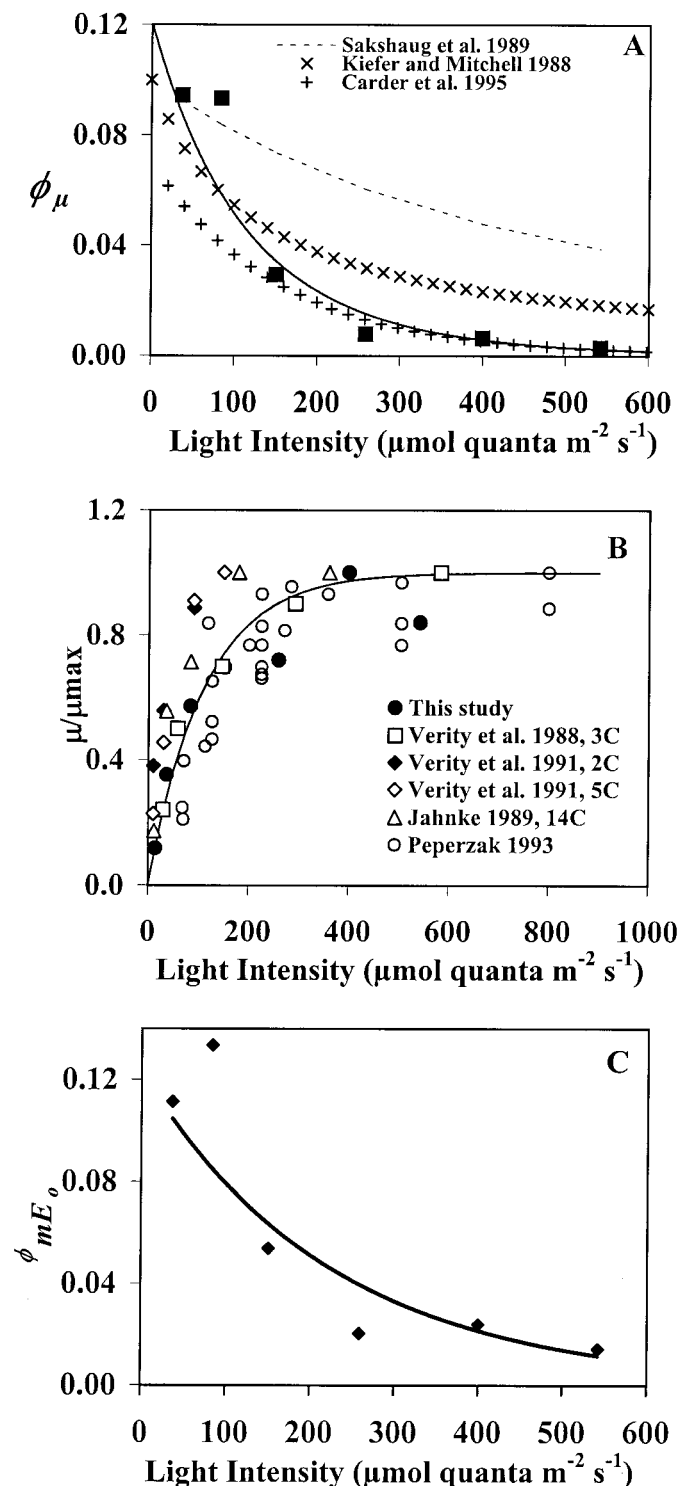


Fig. 8. (A) Light dependence of ϕ_μ (mol C [mol quanta absorbed] $^{-1}$) for *P. antarctica* (squares) using Eq. 10. Our modeled ϕ_μ relationship with light (Eq. 12, solid line) is calculated with $E_{k\mu}$ and ϕ_{mE_o} shown in (B) and (C). This model is compared with the model predictions of Kiefer and Mitchell (1983) where $K_\phi = 120 \mu\text{mol quanta m}^{-2} \text{s}^{-1}$ and the Sakshaug et al. (1989) application of Eq. 11 with a constant $\sigma\tau$ of $1.1 \text{ m}^2 \text{ h (mol photosynthetic unit)}^{-1}$. The ϕ_{max} value is $0.10 \text{ mol C (mol quanta absorbed)}^{-1}$ for the Kiefer and Mitchell and the Sakshaug et al. models. The Carder et al.

tum yields may be more easily attained if one utilizes an environmentally dependent maximal quantum yield, particularly if this can be predicted from knowledge of environmental conditions. For our light-limitation experiment, we define this term as ϕ_{mE_o} . Our expression for the light dependence of ϕ_μ is given by

$$\phi_\mu = \phi_{mE_o} \frac{1 - \exp^{-E_o/E_{k\mu}}}{E_o/E_{k\mu}} \quad (12)$$

By introducing estimates of ϕ_μ , $E_{k\mu}$ ($110 \mu\text{mol quanta m}^{-2} \text{s}^{-1}$; Fig. 8B), and E_o into Eq. 12, we solved for the apparent ϕ_{mE_o} for our cultures whose growth rates were limited by irradiance. Estimated values of ϕ_{mE_o} increased exponentially with decreasing irradiance (Table 2, Fig. 8C) and can be described by the following empirically-derived equation,

$$\phi_{mE_o} = 0.1231e^{-0.0044E_o}, \quad r^2 = 0.83 \quad (13)$$

where E_o is scalar irradiance ($\mu\text{mol quanta m}^{-2} \text{s}^{-1}$). Using $E_{k\mu} = 110 \mu\text{mol quanta m}^{-2} \text{s}^{-1}$ and the ϕ_{mE_o} predicted by Eq. 13, we modeled the light dependence of ϕ_μ using Eq. 12. The modeled ϕ_μ values were close to the experimental ϕ_μ values at all irradiances (Fig. 8A).

Our model parameterization for ϕ_μ , when compared with a model with a hyperbolic function or one that assumes a constant $\sigma\tau$ and ϕ_m (Sakshaug et al. 1989; Carder et al. 1995), improved our ability to fit the rapid decrease of ϕ_μ with E_o (Fig. 8A). Our ϕ_{mE_o} values ranged from 0.012 to 0.11 mol C (mol quanta absorbed) $^{-1}$, in the range of values from previous temperate field studies for maximal quantum yield based on P-E curves and realistic estimates of light absorption (Cleveland et al. 1989; Babin et al. 1996; Sosik 1996). For a *Phaeocystis* bloom, Carder et al. (1995) reported ϕ_m values for photosynthesis that ranged from 0.047 to 0.091 mol C (mol quanta absorbed) $^{-1}$, and Cota et al. (1994) reported an average ϕ_m of $0.1 \pm 0.05 \text{ mol C (mol quanta absorbed)}^{-1}$. An initial attempt to model the data in Fig. 8A using Eq. 11 by setting ϕ_m as a constant and allowing E_k to vary with E_o resulted in unrealistic increases in E_k at low irradiances that were inconsistent with prior reports for the light dependence of P-E relationships. In contrast, holding $E_{k\mu}$ constant, a reasonable approach based on our observations (Fig. 8B), and allowing ϕ_{mE_o} to vary with irradiance provides realistic variability of ϕ_{mE_o} with highest values at low irradiances, which is consistent with prior literature.

Photobiology of Phaeocystis: Implications for its ecology—*Phaeocystis* exhibited a wide range in its ability to harvest light and convert that energy into growth, as shown by the 30-fold range of ϕ_μ in this study. Observations of high $a_{\text{ph}}^*(\lambda)$ and high ϕ_μ have been observed in nature and have resulted in high values of chlorophyll-specific photosynthetic efficiency, chlorophyll-specific assimilation rates, and pri-

←

(1995) model is based on data from a *Phaeocystis* bloom in the North Atlantic. (B) The relationship between relative growth rates of *Phaeocystis* and irradiance. (C) Predicted ϕ_{mE_o} (Eq. 13) with light for our study.

mary productivity during periods of low surface irradiance due to clouds and deep mixed layers (40–60 m) (Smith et al. 1991; Cota et al. 1994). In polar regions, large solar zenith angles, persistent cloud cover, and frequent storms often result in deep mixed layers with low average irradiances (Mitchell 1992). Under these circumstances, a competitive advantage may be gained by maintaining moderate growth rates at low light rather than higher growth rates under more optimal conditions. This hypothesis is corroborated by the observation of early spring blooms of *Phaeocystis* under sea ice (Palmisano et al. 1987; SooHoo et al. 1987; Smith 1996). *Phaeocystis* is also able to tolerate high irradiances and can acclimate to abrupt irradiance changes by xanthophyll cycling, which may in part optimize photosynthesis in fluctuating light environments (Moisan et al. 1998). In addition, it appears that *Phaeocystis* minimizes pigment packaging effects by decreasing the path length of incident light (i.e., cell diameter) while increasing the amount of pigment per cell under low-light acclimation. In addition, the colonial form of *Phaeocystis* offers a size refuge from small grazers without creating the inefficiency of pigment packaging observed in larger diatoms (Riegger and Robinson 1997). The photophysiological characteristics described here suggest that “bottom up” controls contribute in part to the ability of *Phaeocystis* to dominate blooms at times in polar regions.

References

- BABIN, M., A. MOREL, H. CLAUSTRÉ, A. BRICAUD, Z. KOLBER, AND P. G. FALKOWSKI. 1996. Nitrogen- and irradiance-dependent variations of the maximum quantum yield of carbon fixation in eutrophic, mesotrophic and oligotrophic marine systems. *Deep-Sea Res.* **43**: 1241–1272.
- BALCH, W. M., M. R. ABBOTT, AND R. W. EPPLEY. 1989. Remote sensing of primary production—I. A comparison of empirical and semi-analytical algorithms. *Deep-Sea Res.* **36**: 281–295.
- BEHRENFELD, M., AND P. G. FALKOWSKI. 1997. Photosynthetic rates derived from satellite-based chlorophyll concentration. *Limnol. Oceanogr.* **42**: 1–20.
- BAUMANN, M. E. M., C. LANCELOT, F. P. BRANDINI, E. SAKSHAUG, AND D. M. JOHN. 1994. The taxonomic identity of the cosmopolitan prymnesiophyte *Phaeocystis*: A morphological and ecophysiological approach. *J. Mar. Syst.* **5**: 5–22.
- BERNER, T., K. WYMAN, AND P. G. FALKOWSKI. 1989. Photoadaptation and the “package effect” in *Dunaliella tertiolecta* (Chlorophyceae). *J. Phycol.* **25**: 70–78.
- BIDIGARE, B., M. ONDRUSEK, J. MORROW, AND D. A. KIEFER. 1990. In vivo absorption properties of algal pigments. *Ocean Optics 10*, Proc. Society of Photo-Optical Instrumentation Engineers **1302**: 290–302.
- , O. SCHOFIELD, AND B. B. PRÉZELIN. 1989. Influence of zeaxanthin on quantum yield of photosynthesis of *Synechococcus* clone WH7803 (DC2). *Mar. Ecol. Prog. Ser.* **56**: 177–188.
- BUMA, A. G. J., N. BANO, M. J. W. VELDHIJS, AND G. W. KRAAY. 1991. Comparison of the pigmentation of two strains of the prymnesiophyte *Phaeocystis* sp. *Neth. J. Sea Res.* **27**: 173–182.
- CARDER, K. L., Z. P. LEE, J. MARRA, R. G. STEWARD, AND M. J. PERRY. 1995. Calculated quantum yield of photosynthesis of phytoplankton in the marine light-mixed layers (59°N, 21°W). *J. Geophys. Res. Oceans* **100**: 6655–6663.
- CHARLSON, R. J., J. E. LOVELOCK, M. O. ANDREAEE, AND S. G. WARREN. 1987. Oceanic phytoplankton, atmospheric sulphur, cloud albedo, and climate. *Nature* **326**: 655–661.
- CLEVELAND, J. S., AND M. J. PERRY. 1987. Quantum yield, relative specific absorption and fluorescence in nitrogen-limited *Chaetoceros gracilis*. *Mar. Biol.* **94**: 489–497.
- , D. A. KIEFER, AND M. C. TALBOT. 1989. Maximum quantum yield of photosynthesis in the northwestern Sargasso Sea. *J. Mar. Res.* **47**: 869–892.
- COTA, G. A., W. O. SMITH, AND B. G. MITCHELL. 1994. Photosynthesis of *Phaeocystis* in the Greenland Sea. *Limnol. Oceanogr.* **39**: 948–953.
- CULLEN, J. J. 1990. On models of growth and photosynthesis in phytoplankton. *Deep-Sea Res.* **37**: 667–783.
- DUBINSKY, Z., P. G. FALKOWSKI, AND K. WYMAN. 1986. Light harvesting and utilization by phytoplankton. *Plant Cell Physiol.* **27**: 1335–1349.
- FALKOWSKI, P. G., AND J. A. RAVEN. 1997. *Aquatic photosynthesis*. Blackwell.
- FRYXELL, G. A., AND G. A. KENDRICK. 1983. Austral spring microalgae across the Weddell Sea ice edge: Spatial relationships found along a northward transect during AMERIEZ 83. *Deep-Sea Res.* **35**: 1–20.
- GIBBS, S. P. 1970. The comparative ultrastructure of the algal chloroplast. *Ann. N.Y. Acad. Sci.* **175**: 454–473.
- GUILLARD, R. R. L., AND J. H. RYTHER. 1962. Studies on marine planktonic diatoms. I. *Cyclotella nana* Hustedt and *Detonula confervacea* (Cleve) Gran. *Can. J. Microbiol.* **8**: 229–239.
- HAXO, F. T., AND L. R. BLINKS. 1950. Photosynthetic action spectra of marine algae. *J. Gen. Physiol.* **33**: 389–422.
- JAHNKE, J. 1989. The light and temperature dependence of growth rate and elemental composition of *Phaeocystis globosa* Scherffel and *P. pouchetii* (Har.) Lagerh. in batch cultures. *Netherlands J. Sea Res.* **1**: 15–21.
- JEFFREY, S. W., AND G. M. HALLEGRAEFF. 1987. Chlorophyllase distribution in ten classes of phytoplankton: A problem for chlorophyll analysis. *Mar. Ecol. Prog. Ser.* **35**: 293–304.
- JOHNSON, G., N. B. NELSON, R. V. M. JOVINE, AND B. B. PRÉZELIN. 1994. Chromoprotein- and pigment-dependent modeling of spectral light absorption of two dinoflagellates, *Prorocentrum minimum* and *Heterocapsa pygmaea*. *Mar. Ecol. Prog. Ser.* **114**: 245–258.
- KIEFER, D. A., AND B. G. MITCHELL. 1983. A simple steady state description of phytoplankton growth based on absorption cross section and quantum efficiency. *Limnol. Oceanogr.* **28**: 770–776.
- KIRK, J. T. O. 1976. A theoretical analysis of the contribution of algal cells to the attenuation of light within natural waters. III. Cylindrical and spheroidal cells. *New Phytol.* **77**: 341–358.
- . 1994. *Light and photosynthesis in aquatic ecosystems*. Cambridge Univ. Press.
- KOPF, U., AND J. HEINZ. 1984. 2,7-Bis (diethylamino) phenazonium chloride as a quantum counter for emission measurements between 240 and 700 nm. *Anal. Chem.* **56**: 1931–1935.
- LISS, P. S., G. MALIN, S. M. TURNER, AND P. M. HOLLIGAN. 1994. Dimethyl sulphide and *Phaeocystis*: A review. *J. Mar. Syst.* **5**: 41–53.
- MAUZERALL, D. 1978. Multiple excitations and the yield of chlorophyll *a* fluorescence in photosynthetic systems. *Photochem. Photobiol.* **28**: 991–998.
- MITCHELL, B. G. 1992. Predictive bio-optical relationships for polar oceans and marginal ice zones. *J. Mar. Syst.* **3**: 91–105.
- , AND D. A. KIEFER. 1988. Chlorophyll *a* specific-absorption and fluorescence excitation spectra for light-limited phytoplankton. *Deep-Sea Res.* **35**: 639–663.
- MOISAN, T. A., M. OLAIZOLA, AND B. G. MITCHELL. 1998. Xanthophyll cycling in *Phaeocystis*: Changes in cellular absorption,

- fluorescence and photoprotection. *Mar. Ecol. Prog. Ser.* **169**: 113–121.
- MOREL, A., AND A. BRICAUD. 1986. Inherent optical properties of algal cells including picoplankton: Theoretical and experimental results. *Can. Bull. Fish. Aquat. Sci.* **214**: 521–559.
- NELSON, N. B., AND B. B. PRÉZELIN. 1990. Chromatic light effects and physiological modeling of absorption properties of *Heterocapsa pygmaea* (*Glenodinium* sp.). *Mar. Ecol. Prog. Ser.* **63**: 37–46.
- NEORI, A., M. VERNET, O. HOLM-HANSEN, AND F. T. HAXO. 1988. Excitation spectra of chlorophyll far-red fluorescence compared to chlorophyll red fluorescence and to photosystem II photosynthetic action spectra in algae. *Mar. Ecol. Prog. Ser.* **44**: 297–302.
- OWENS, T. G. 1991. Energy transformation and fluorescence in photosynthesis. *NATO Adv. Sci. Ser.* **27**: 101–137.
- PALMISANO, A. C., J. B. SOOHOO, R. L. MOE, AND C. W. SULLIVAN. 1987. Sea ice microbial communities. VII. Changes in under-ice spectral irradiance during the development of Antarctic sea ice microalgal communities. *Mar. Ecol. Prog. Ser.* **35**: 165–173.
- PEPERZAK, L. 1993. Daily irradiance governs growth rate and colony formation of *Phaeocystis* (Prymnesiophyceae). *J. Plankton Res.* **15**: 809–821.
- RIEGGER, L., AND D. ROBINSON. 1997. Photoinduction of UV-absorbing compounds in Antarctic diatoms and *Phaeocystis antarctica*. *Mar. Ecol. Prog. Ser.* **160**: 13–25.
- ROUSSEAU, V., D. VAULOT, R. CASOTTI, V. CARIOU, J. LENZ, J. GUNKEL, AND M. BAUMANN. 1994. The life cycle of *Phaeocystis* (Prymnesiophyceae): Evidence and hypotheses. *J. Mar. Syst.* **5**: 23–39.
- SAKSHAUG, E., K. ANDRESEN, AND D. A. KIEFER. 1989. A steady state description of growth and light absorption in the marine planktonic diatom *Skeletonema costatum*. *Limnol. Oceanogr.* **34**: 198–205.
- , G. JOHNSEN, K. ANDRESEN, AND M. VERNET. 1991. Modeling of light-dependent algal photosynthesis and growth: Experiments with the Barents Sea diatoms *Thalassiosira nordenskiöldii* and *Chaetoceros furcellatus*. *Deep-Sea Res.* **38**: 415–430.
- SMITH, W. O. 1996. Phytoplankton biomass and productivity in the Ross Sea polynya during November–December, 1994. *EOS Trans. Am. Geophys. Union (Ocean Sci. Meet. Suppl.)* **76**: OS32M–OS33M.
- , L. A. CODISPOTI, D. M. NELSON, T. MANLEY, E. J. BUSKEY, H. J. NIEBAUER, AND G. F. COTA. 1991. Importance of *Phaeocystis* blooms in the high-latitude ocean carbon cycle. *Nature* **352**: 514–516.
- SOOHOO, J. B., A. C. PALMISANO, S. T. KOTTMEIER, M. P. LIZOTTE, S. L. SOOHOO, AND C. W. SULLIVAN. 1987. Spectral light absorption and quantum yield of photosynthesis in sea ice microalgae and a bloom of *Phaeocystis pouchetii* from McMurdo Sound, Antarctica. *Mar. Ecol. Prog. Ser.* **39**: 175–189.
- SOSIK, H. M. 1996. Bio-optical modeling of primary production: Consequences of variability in quantum yield and specific absorption. *Mar. Ecol. Prog. Ser.* **143**: 225–238.
- , AND B. G. MITCHELL. 1991. Absorption, fluorescence and quantum yield for growth in nitrogen limited *Dunaliella tertiolecta*. *Limnol. Oceanogr.* **36**: 910–921.
- , AND ———. 1995. Absorption by phytoplankton, photosynthetic pigments, and detritus in the California Current System. *Deep-Sea Res.* **42**: 1717–1748.
- STOECKER, D. K., M. PUTT, AND T. A. MOISAN. 1996. Nano- and microplankton dynamics during the spring *Phaeocystis* sp. bloom in McMurdo Sound, Antarctica. *J. Mar. Biol. Assoc. U.K.* **75**: 815–832.
- VAN BOECKEL, W. H. M., F. C. HANSEN, R. RIEGMAN, AND R. BAK. 1992. Lysis-induced decline of a *Phaeocystis* spring bloom and coupling with the microbial food web. *Mar. Ecol. Prog. Ser.* **81**: 269–276.
- VAULOT, D., J. BIRRIEN, D. MARIE, R. CASOTTI, M. J. W. VELDHUIS, G. W. KRAAY AND M. CHRÉTIENNOT-DINET. 1994. Morphology, ploidy, pigment composition, and genome size of cultured strains of *Phaeocystis* (Prymnesiophyceae). *J. Phycol.* **30**: 1022–1035.
- VERITY, P. G., T. J. SMAYDA, AND E. SAKSHAUG. 1991. Photosynthesis, excretion, and growth rates of *Phaeocystis* colonies and solitary cells, p. 117–128. *In* E. Sakshaug, C. C. E. Hopkins, and N. A. Øritsland [eds.], *Proceedings of the Pro Mare Symposium on Polar Marine Ecology*, Trondheim, 12–16 May 1990.
- , T. A. VILLAREAL, AND T. J. SMAYDA. 1988. Ecological investigations of blooms of colonial *Phaeocystis pouchetii*. I. Abundance, biochemical composition, and metabolic rates. *J. Plankton Res.* **10**: 219–248.
- WASSMAN, P., M. VERNET, B. G. MITCHELL, AND F. REY. 1990. Mass sedimentation of *Phaeocystis pouchetii* in the Barents Sea. *Mar. Ecol. Prog. Ser.* **66**: 183–195.
- WEISSE, T., K. TANDE, P. VERITY, F. HANSEN, AND W. GIESKES. 1994. The trophic significance of *Phaeocystis* blooms. *J. Mar. Syst.* **5**: 67–79.
- WRIGHT, S. W., S. W. JEFFREY, R. F. C. MANTOURA, C. A. LLEWELLYN, T. BJÖRNLAND, D. REPETA, AND N. WELSCHMEYER. 1991. Improved HPLC method for the analysis of chlorophylls and carotenoids from marine phytoplankton. *Mar. Ecol. Prog. Ser.* **77**: 183–196.
- YENTSCH, C. S., AND D. W. MENZEL. 1963. A method of the determination of phytoplankton chlorophyll and phaeophytin by fluorescence. *Deep-Sea Res.* **10**: 221–231.

Received: 21 July 1997

Accepted: 4 September 1998

Amended: 23 October 1998